Original Paper

Indoor+Built Environment

Indoor Built Environ 1998;7:276–288

Accepted: September 6, 1998

W.K. Chow
L.T. Wong

Department of Building Services Engineering, The Hong Kong Polytechnic University, Hong Kong, China

Equations for a Ventilation Design Derived from Computational Fluid Dynamics

Key Words
Computational fluid dynamics
Ventilation

Abstract
Computational fluid dynamics (CFD) was used in a study of the air flow characteristics in the occupied building zone. Correlation equations between the mean air speeds and the percentage dissatisfied with the macroscopic flow numbers were derived. Ten macroscopic flow numbers including the total ventilation rate, the air change rate, ventilation rate, air diffusion performance index, modified jet momentum number, two new flow numbers and three expressions of jet momentum ratio were investigated. A total number of 25 numerical experiments under isothermal flow conditions with four different geometrical arrangements (labelled A–D) were performed. The correlation equations derived from CFD were compared with those obtained from experimental studies. It is found that the jet momentum ratio R_{M2} gives the equation with the best correlation coefficient and so is recommended for ventilation design.

Introduction

Macroscopic flow numbers commonly used in ventilation design such as the air change rate (number of air changes per hour, ACH) and the ventilation rate [1–6] are not good enough for specifying indoor air flow characteristics. The results do not correlate well with the indoor environmental conditions such as the air speed distribution and the percentage of people dissatisfied with the air draught in the occupied zone. One of the reasons is that most of those flow numbers do not include the geometry of the enclosure and the locations of air diffusers [7].

Air speeds in the occupied zone depend on the inlet jet momentum of the air diffusion devices [8, 9]. Three jet momentum ratios, R_{M1}, R_{M2}, and R_{M3}, and two newly introduced flow numbers, X_1 and X_2, are proposed to specify the ventilation design by including the effects of the geometry of the rooms and the location of air diffusers [10–14]. Correlation equations [11] relating the mean air speeds and the percentage of people dissatisfied (PD) [15] in the occupied zone with these flow numbers are shown to be useful for design purposes.

Deriving correlation equations by physical models is good but far too expensive. As an alternative the powerful design tool computation fluid dynamics (CFD) [16–18] can now be applied to derive such correlation equations. However, there are problems in applying CFD models for the simulation of indoor air flow [17, 18]. Usually, training is required to use the software even with commercial packages. Keying in the input parameters and setting up a mesh system for the building takes time. The boundary conditions such as the parameters for the air supply inlet

KARGER
Fax +41 61 306 12 34
E-Mail karger@karger.ch
www.karger.com

1420–326X/98/0076–0276$17.50/0

Accessible online at:
http://BioMedNet.com/karger

Prof. W.K. Chow
Department of Building Services Engineering, The Hong Kong Polytechnic University
Hung Hom, Kowloon, Hong Kong (China)
Tel. +852 2766 5843, Fax +852 2774 6146
E-Mail bewkchow@polyu.edu.hk

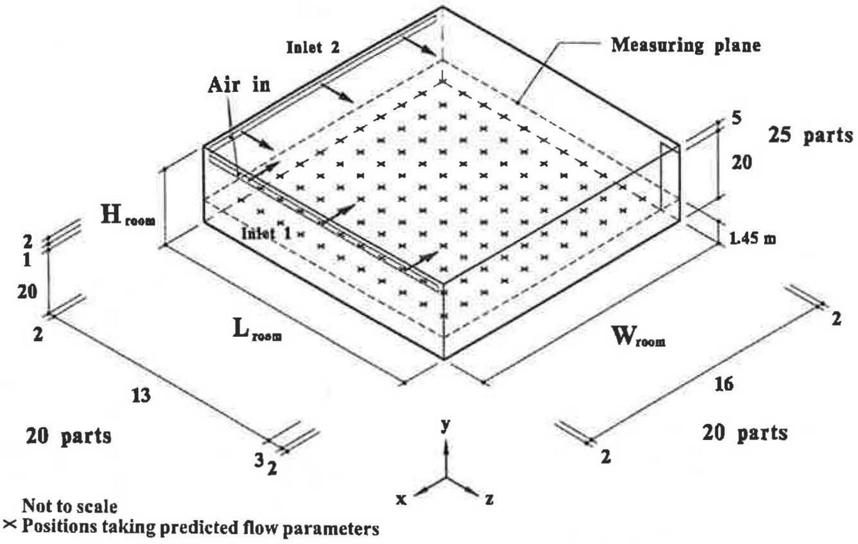

Fig. 1. Configurations of testing site of numerical experiments for flow conditions A, B and C (total of 18 flow conditions).

and free boundaries have to be specified carefully. A large volume of output data on the velocity components, temperature and turbulent parameters is obtained. This is generally more than sufficient as only 10% of the data have direct application, the rest are used for checking the results. Nevertheless, CFD can be a powerful tool for studying indoor air flow if the results of simulations are considered carefully together with results from experimental studies. Using the method to derive correlation equations for ventilation design is a good use of the technique and the object of this paper is to illustrate this new application.

Correlation equations involving local mean air speed, U_p and PD, with 10 flow numbers [9–13] are derived using CFD. The 10 flow numbers are: the total ventilation rate, Q; ACH; the ventilation rate per unit floor area, VR; the air diffusion performance index, ADPI; the modified jet momentum number, J* [10, 11]; the new flow numbers X_1 and X_2 [12], and the 3 jet momentum ratios R_{M1}, R_{M2} and R_{M3} [12, 13]. Results are compared with those determined by physical models reported earlier [9–13].

Methods

Sites for Numerical Experiments

The sites selected for the numerical experiments all have 2 high-level wall-mounted air supply inlets, which is a common ventilation design in the Hong Kong Special Administrative Region (HKSAR, formerly Hong Kong) for a room height between 3 and 5 m [7]. Four different geometrical arrangements with different aspect ratios and locations of air supply inlets labelled A–D were considered. The configurations for simulations A–C are shown in figure 1, and the geometry for simulation D is shown in figure 2. The physical dimensions of the rooms and locations of the air supply inlets are summarized in table 1. Two air supply inlets at right angles to each other were installed at a high level. Different air supply inlet flow rates (determined by the ACH) were considered.

High as well as low values of ACH were tested because a recent survey [7, 9] of local ventilation systems illustrated that the ACH could be as high as 200 as in table 2. Criteria recommended by common design guides for the ventilated spaces [1, 3] are included as well for comparison.

The ACH of an application would be higher for smaller volume spaces. For example, up to 180 ACH was measured in an office smaller than 100 m^3, but only 8.5 ACH in those with volumes bigger than 1,000 m^3. Rates above 200 ACH were recorded for small toilets of 10 m^3, but for bigger toilets above 50 m^3 they were only 6 ACH. One reason for this is a lower limit on the manufactured duct size. Further, no special equipment has been designed for small rooms and so standard products available in the marketplace were selected. A fan coil unit with a supply flow rate of 0.3 $m^3 \cdot s^{-1}$ installed in an office of a volume of 20 m^3 would give 54 ACH. Partitioning a small office which had an air inlet with a high flow rate supply would give an even higher ACH.

Geometry and Flow Conditions for the Four Sets of Simulations

Simulation A. A square room of 18.4 m × 18.4 m and 5 m high was considered. There were 6 flow conditions labelled A1–A6 for which the air supply inlet velocities varied from 1 to 3 $m \cdot s^{-1}$. The ACH supplied to the room were from 11.61 to 23.22.

Simulation B. The floor area of the room was the same as that for simulation A but the room height was lower at 3.5 m. Six flow conditions B1–B6 with the same air supply inlet velocities as A1–A6 were used. Note that reducing the room height leads to higher ACH, and

Table 1. Configuration of sites for numerical experiment

A Simulations

Simulations	Dimensions of sites simulated					Inlet dimensions					Exhaust dimensions		
	length L_{room} m	width W_{room} m	height H_{room} m	area A_{room} m^2	volume V_{room} m^3	number of inlets N_{in}	length L_{in}, m	height H_{in} m	installed height H_b, m	area A_{in} m^2	length L_{ou} m	height H_{ou} m	area A_{ou} m^2
A	18.4	18.4	5	339	1,693	2	18.2	0.1	4.88	3.64	1.45	4.45	6.5
B	18.4	18.4	3.5	339	1,198	2	18.2	0.1	3.41	3.64	1.45	3.18	4.60
C	18.4	12.4	3.5	228	807	2	18.2/12.2	0.1	3.41	3	1.45	3.18	4.60
D	18.4	18.4	5	339	1,693	2	18.2/9.1	0.1	4.88	2.7	1.45	4.45	6.45

B Flow conditions

Flow conditions	Inlet conditions				Distance between		
	inlet 1 velocity U_{in1}, m s^{-1}	inlet 2 velocity U_{in2}, m s^{-1}	mean inlet velocity U_{in}, m s^{-1}	spacing S_d, m	inlets and measured plane D_{ip}, m	outlet and measured plane D_{op}, m	inlets and outlet D_{io}, m
A1	3.0	3.0	3.00				
A2	2.5	2.5	2.50				
A3	2.0	2.0	2.00	14.27	7.38	12.53	19.20
A4	1.0	3.0	2.00				
A5	1.5	1.5	1.50				
A6	1.0	2.0	1.50				
B1	3.0	3.0	3.00				
B2	2.5	2.5	2.50				
B3	2.0	2.0	2.00	14.27	6.80	12.53	19.10
B4	1.0	3.0	2.00				
B5	1.5	1.5	1.50				
B6	1.0	2.0	1.50				
C1	3.0	3.0	3.00				
C2	2.5	2.5	2.50				
C3	1.0	3.0	2.20	12.07	5.90	10.71	16.35
C4	2.0	2.0	2.00				
C5	1.0	2.0	1.60				
C6	1.5	1.5	1.50				
D1	3.0	2.0	2.67	17.32	6.22		17.64
D2	2.0	2.0	2.00	17.32	6.22		17.64
D3	1.5	2.0	1.67	11.07	6.22		17.64
D4	1.5	1.5	1.50	11.07	8.97	12.53	20.90
D5	1.0	2.0	1.33	17.32	8.97		20.90
D6	1.0	2.0	1.33	11.07	8.97		20.90
D7	1.5	1.0	1.33	11.07	8.97		20.90

the modified jet momentum number J* and the jet momentum ratios R_{M1}, R_{M2} and R_{M3} are also changed.

Simulation C. A rectangular room of 18.4 m × 12.4 m with a height of 3.5 m was considered. Flow conditions were labelled C1–C6 with air supply inlet velocities the same as A1–A6. The details are shown in table 1.

Simulation D. The geometry for this simulation was the same as those for simulation A, except that a half-room length air supply inlet and a full-room length air supply inlet were installed as shown in figure 2. Seven flow conditions labelled from D1 to D7 were examined with two different locations of the half-room length air supply inlet at different supply flow rates. The configurations, air supply inlet flow rates, inlet locations and parameters for the 7 flow conditions are shown in table 1.

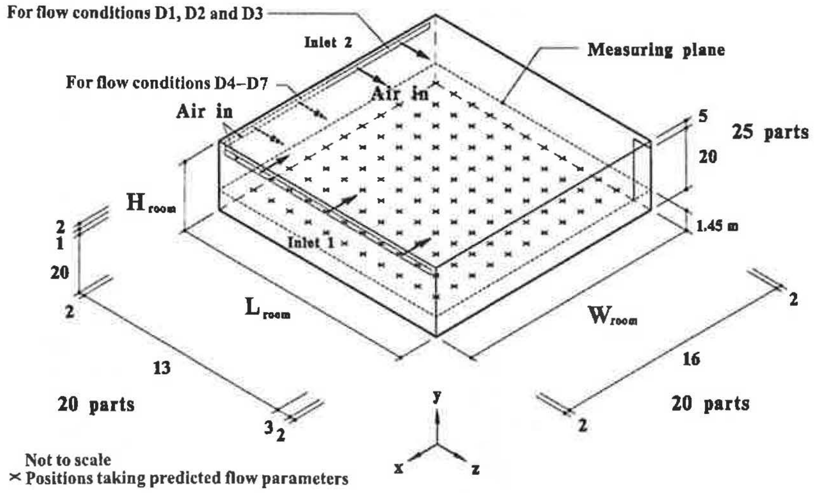

Fig. 2. Configurations of testing site of numerical experiments for flow conditions D (7 flow conditions).

Table 2. Examples of designed ACH

Application	Local examples [7, 9] space volume m^3	Local examples [7, 9] ACH	ASHRAE [3] ACH	CIBSE [1] ACH
Transportation terminals	≤ 3,000	2–22	8–12	–
Conference rooms	20–200	6–30	–	6–10
Dining halls, restaurants	2,000	6–10	8–12	10–15
Garages	varies	4–6	4–6	6–10
Kitchens	varies	40–60	12–15	20
Lavatories and toilets	10–50	30–200	–	≥ 5
	≥ 50	6–20	–	≥ 5
Exhibition halls	500–4,000	5–10	8–12	3–4
Office	< 100	5–180		
	100–1,000	7.5–30	4–10	4–6
	> 1,000	8.5		
Shops, department stores, supermarkets	100–5,000	2–11	–	based on heating or cooling loads
Studios	–	–	15–40	

Computational Fluid Dynamics

The CFD code used in this study was developed by Chow [19, 20] and has been applied to the simulation of indoor air motion [7, 18–20] induced by thermal sources such as fire, heating, ventilation and air-conditioning systems. For the present application a set of equations describing conservation of mass, momentum and energy was set up. Reynolds (time) averaging was performed to transform this set of governing equations from instantaneous values into mean values.

Characteristics of the CFD package are:

- use of turbulence models such as the two-equation k-ε turbulence model;
- control volume method to discretize the set of conservation equations;
- algorithms for solving the pressure-velocity-linked equations such as SIMPLER or PISO.

A non-uniform mesh system (25 × 25 × 20) along the x, y, z directions of a Cartesian co-ordinate system as shown in figures 1 and 2 was set up for all simulations. The wall boundaries were assumed to be adiabatic and a standard wall function was adopted. This assumption is valid for applying CFD to the design of ventilation systems in the HKSAR because of the small changes in outdoor temperature during daytime office hours [7]. Velocity and other scalar quantities were specified at the free boundary outlet corresponding to the air supply inlets.

Room enclosures were assumed to be empty for studying the relationship between the air speed distribution, percentage of thermal discomfort using the PD_{50} and the macroscopic flow numbers.

Physical Measurements

Experimental data had been measured previously in an air flow chamber under 5 flow conditions and in 7 railway waiting halls [7, 10, 11]. These data were used to assess the correlation equations derived from CFD. The air speeds measured at locations in those spaces were recorded and used in the CFD calculations to calculate the room mean air speed.

Chamber Measurements. Indoor air flow characteristics [10] in an air-conditioned environmental chamber of size 4.1 × 2.6 × 2.1 m (height) were studied experimentally. Five flow conditions, 2 with a high-sidewall grille and 3 with a high-sidewall opening (without diffuser) were studied. Hot-wire anemometers [21] used in the study were tungsten probes of a diameter of 5 µm and an electrical resistance of 15 Ω. They were calibrated in a wind tunnel placed inside a climate chamber under controlled conditions. The measurement errors of the instrument were 20% at an air speed of 0.05 $m \cdot s^{-1}$, 10% at 0.1 $m \cdot s^{-1}$ and 5% at 0.2 $m \cdot s^{-1}$. The uncertainties of measuring the mean air speeds were ± 20.9% at an air speed 0.05 $m \cdot s^{-1}$, ± 11.7% at 0.1 $m \cdot s^{-1}$ and ± 7.8% at 0.2 $m \cdot s^{-1}$. Air speeds inside the chamber were measured by hot-wire anemometers at 109 positions. At each position, a 3-min measurement was taken. The air temperature and relative humidity were measured by thermocouples and aspiration psychrometers, respectively, to the nearest 0.5°C. Thermal comfort was evaluated using an ADPI and the PD. Macroscopic numbers describing indoor air flow including the Archimedes number, the Reynolds number and the jet momentum number were measured. Variations in these thermal comfort indices for different values of the macroscopic physical numbers for the air flow under isothermal conditions were examined and empirical corrections derived.

Measurements in Railway Waiting Rooms. Air speeds induced by mechanical ventilation at the occupied zone were studied experimentally at 7 railway stations in the HKSAR [11]. A Brüel & Kjær (Nærum, Denmark) indoor climate analyser type 1213 [22] was used to measure the air speeds at different positions at 1.45 m above floor level. The instrument employed an omni-dimensional hot-wire anemometer to determine the air speed. The measurement error of the instrument was 0.05 $m \cdot s^{-1}$ at an air speed between 0.05 and 1 $m \cdot s^{-1}$. The uncertainties of measuring mean air speeds were ± 25.5% at 0.2 $m \cdot s^{-1}$ and ± 11.2% at 0.5 $m \cdot s^{-1}$. The air speed contours and turbulence intensity were calculated. Macroscopic numbers describing air flow in the space including the Reynolds number and the jet momentum number were estimated and their potential application examined.

Indoor Air Flow Characteristics

The mean air speed, U_p and the PD with the air draught at the occupied zone [15] are the two key parameters in specifying the indoor air flow characteristics. They are calculated from the predicted flow fields at a plane 1.45 m above the floor. The justification for using a single measuring plane for evaluating air flow conditions in the occupied zone has been made and reported previously [11].

The mean air speed U_p at a grid point p (x, y, z) was calculated from the mean air velocity components given by u_p, v_p and w_p at that point. Perfect mixing was assumed so that the control volume τ_p of the point p has a mean air speed U_p given by:

$$U_p = \sqrt{u_p^2 + v_p^2 + w_p^2} \tag{1}$$

The mean air speed of the occupied zone U_{room} is the averaged value over all the points p (which depends on the grid system) in that zone:

$$U_{room} = \frac{\Sigma\, U_p \cdot \tau_p}{\Sigma\, \tau_p} \tag{2}$$

The PD with the air draught in an environment was calculated in terms of the mean air speed U_p, the turbulence intensity Tu and the air temperature T_a [15]:

$$PD = (3.143 + 0.3696\, U_p\, Tu)\,(34 - T_a)\,(U_p - 0.05)^{0.6223} \tag{3}$$

In this equation, the mean air speed is taken to be 0.05 $m \cdot s^{-1}$ when it is less than 0.05 $m \cdot s^{-1}$, and PD is taken to be 100% if the value is higher than 100%.

Note that values for both U_p and PD would be different at different locations. Their median values U_{50} and PD_{50} are calculated for further analysis.

Macroscopic Flow Numbers

Macroscopic flow parameters [1–7] including the total ventilation rate Q, the ACH, the VR, the ADPI and the modified jet momentum number J* are considered in this paper. Reviews of these expressions and their potential application have been reported earlier [7, 11] and are not repeated here. Values of the ADPI were determined from the predicted local air speed at a constant temperature of 26°C.

Macroscopic flow numbers related to the jet momentum ($U_{in} \cdot A_{in}$, where U_{in} is the inlet air jet velocity and A_{in} is the cross-sectional area of the inlet) of the air supply inlet have been investigated. Three expressions for the jet momentum ratios R_{M1}, R_{M2} and R_{M3} which were defined by using different values of streamwise length derived by considering the distance between the inlet and outlet D_{io}, the distance between the inlet and occupied zone D_{ip}, and the distance between the outlet and occupied zone D_{op} have been calculated [12–14, 23]:

$$R_{M1} = \frac{U_{in}^2 \cdot A_{in}}{D_{io}} \tag{4}$$

$$R_{M2} = \frac{U_{in}^2 \cdot A_{in}}{D_{ip} + D_{op}} \tag{5}$$

$$R_{M3} = \frac{U_{in}^2 \cdot A_{in}}{(D_{ip} + D_{op})^2} \tag{6}$$

The distance between the air supply inlet and the measured plane, D_{ip}, was defined as the distance between the mean location of the air supply inlets to the centre point on the measuring plane.

A new flow number X_1 defined by considering the relative value of the range R to be distributed by a diffuser and the separation spacing S_d between the air supply inlets has been proposed [12]. The range R depends on the temperature of the air discharged and would be different for ceiling diffusers and linear diffusers. For air discharging at a temperature very close to the ambient one, the range can be approximated by the equation for the trajectory of a free particle under gravity:

$$R \approx U_{in} \sqrt{\frac{2H_b}{g}} \tag{7}$$

where H_b is the height of the diffuser above the floor level.

Table 3. Numerical experiments

		Flow conditions				
		Al, A2	A3–A6	B1–B6	C1–C6	D1–D7
Dimensions		three-dimensional				
Turbulent model		two-equation k-ε model				
Computational grid		non-uniform, finer grids near walls				
Mesh size	Length	20				
	Width	20				
	Height	25				
Number of cells		10,000				
Boundary conditions		referred to figures 1 and 2				
Difference scheme		power law				
Relaxation technique		under relaxation scheme				
Algorithm used in solving the pressure-velocity-linked equations		PISO				
Computer system		VAX6500	Pentium 133			
Time step		0.1 s				
Computational time		approx. 24 h	approx. 5.5 h			

The flow number X_1 can be defined by the ratio of R to S_d, keeping the other parameters constant:

$$X_1 = \frac{U_{in}}{S_d}\sqrt{\frac{H_b}{g}} \qquad (8)$$

The separation distance (spacing) between the air supply inlets S_d taken as the average distance between the air supply inlets can be calculated by the following equation and is shown in table 1.

$$S_d = \frac{\int_{z_1}^{z_2}\int_{x_1}^{x_2}(x^2 + z^2)dx \cdot dz}{(z_2-z_1)(x_2-x_1)} \qquad (9)$$

It is expected that the larger the X_1 number, the shorter will be the value of S_d with respect to the range R and so a higher value of U_{50} will result. The values of S_d were calculated from the above equation and are shown together with X_1 in table 1.

Another flow number X_2 was also proposed by considering the trajectory equation reported in the literature [14, 23]. An equation relating the horizontal distance z from the jet to the vertical distance x was found:

$$z \approx \frac{x^3}{U_{in}^2} \qquad (10)$$

The flow number X_2 can be derived by taking x to be the height H_b of the air supply inlet above the ground level:

$$X_2 = \frac{H_b^3}{S_d\, U_{in}^2} \qquad (11)$$

Results

Numerical experiments of four defined simulations under 25 flow conditions were performed either on a VAX-Cluster mini-supercomputer system or on a Pentium personal computer. The CPU time for the simulations with a mesh size of 10,000, simulation time 150 s and time step 0.1 s was 24 h on the VAX-Cluster system and 5.5 h on the personal Pentium computer. A summary of the computing details is shown in table 3. The output data files were processed graphically using a personal computer with a package developed in-house for plotting velocity vectors and temperature contours.

All the macroscopic numbers calculated from the predicted flow fields for the 25 numerical experiments are shown in table 4.

Typical examples (for flow condition Al) on the flow field at 150 s are shown in figure 3a–d for the planes at i = 5, 15, j = 9, 21 and k = 5, 10, 15. Predicted mean air speeds U_p and PD contours at 1.45 m above the floor level are shown in figure 4a and b which describes the indoor air flow characteristics of the enclosures.

In addition, the spatial distributions based on the mean air speeds U_p and the PD represented by calculating the first quartile (U_{25}, PD_{25}), median (U_{50}, PD_{50}) and third quartile (U_{75}, PD_{75}) values of the data taking on the plane 1.45 m above the floor level are shown in table 4.

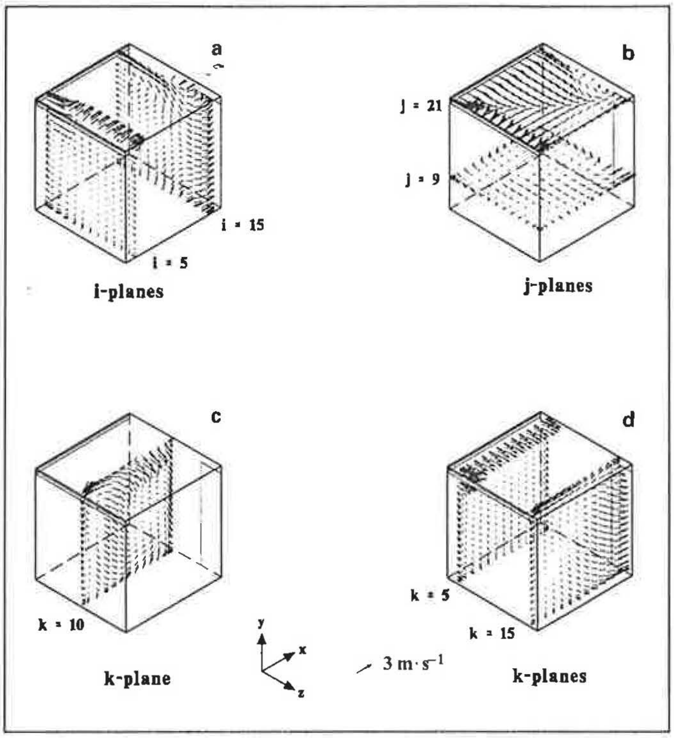

Fig. 3. Simulated flow field for flow condition A1.

Correlation Equations for Ventilation Design

Correlation equations between the mean air speeds U_{room}, U_{50} and PD_{50} with the macroscopic flow numbers ACH, VR, J*, X_1, X_2, R_{M1}, R_{M2} and R_{M3} in the 25 numerical experiments were derived using the method of least square fitting. The results are shown in table 5 together with the correlation coefficients. From the correlation coefficients, the equations were graded as good, fair, poor and unphysical. In addition to linear equations, non-linear equations were considered for some cases.

The equations were also compared with those U_{room}, and U_{50} deduced experimentally in the environmental chamber and the mechanically ventilated spaces. The correlation equations are shown in table 6.

The predicted median value of the mean air speeds U_{50} was related to the number of air changes per hour, ACH as shown in table 5. The selected range of ACH (from 7.7 to 41 ACH) is the normal design range used in industry. It is observed that air speeds increased as the ACH increased. Since the ACH depends on the room volume but not on its geometry, the predicted result did not match the experimental data measured obtained from buildings of different geometry and sizes. The same results were found for

Table 4. Macroscopic flow numbers and predicted results

Flow conditions	Total ventilation flow rate Q $m^3 \cdot s^{-1}$	Air change rate ACH $n \cdot h^{-1}$	Ventilation rate VR $dm^3 \cdot s^{-1} \cdot m^{-2}$	ADPI %	Modified jet momentum number J* n	Flow number X_1 n	X_2 n	Jet momentum ratio R_{M1} $m^3 \cdot s^{-2}$	R_{M2} $m^3 \cdot s^{-2}$	R_{M3} $m^2 \cdot s^{-2}$	Room mean velocity U_{room} $m \cdot s^{-1}$	Room air speeds U_{25} $m \cdot s^{-1}$	U_{50} $m \cdot s^{-1}$	U_{75} $m \cdot s^{-1}$	Percentage dissatisfied [15] PD_{25} %	PD_{50} %	PD_{75} %
A1	10.92	23.22	32.25	2	0.00202	0.148	0.902	1.706	1.646	0.0827	0.655	0.489	0.594	0.800	15.1	17.2	21.0
A2	9.10	19.35	26.88	13	0.00141	0.124	1.299	1.185	1.143	0.0574	0.555	0.394	0.518	0.685	12.9	15.7	19.0
A3	7.28	15.48	21.50	35	0.00090	0.099	2.030	0.758	0.731	0.0367	0.441	0.301	0.406	0.579	10.6	13.2	16.9
A4	7.28	15.48	21.50	16	0.00090	0.099	2.030	0.758	0.731	0.0367	0.540	0.408	0.511	0.669	10.4	12.1	14.6
A5	5.46	11.61	16.13	60	0.00051	0.074	3.610	0.427	0.411	0.0207	0.292	0.186	0.277	0.412	7.3	10.0	13.4
A6	5.46	11.61	16.13	59	0.00051	0.074	3.610	0.427	0.411	0.0207	0.304	0.170	0.300	0.424	5.5	8.4	10.6
B1	10.92	32.82	32.25	29	0.00289	0.124	0.310	1.715	1.695	0.0877	0.544	0.315	0.562	0.737	8.1	12.2	14.7
B2	9.10	27.35	26.88	37	0.00201	0.103	0.446	1.191	1.177	0.0609	0.460	0.241	0.430	0.667	6.7	10.3	13.9
B3	7.28	21.88	21.50	57	0.00128	0.083	0.696	0.762	0.753	0.0390	0.372	0.240	0.286	0.517	6.8	7.8	11.8
B4	7.28	21.88	21.50	23	0.00128	0.083	0.696	0.762	0.753	0.0390	0.494	0.371	0.510	0.626	9.3	11.7	13.5
B5	5.46	16.41	16.13	69	0.00072	0.062	1.238	0.429	0.424	0.0219	0.282	0.174	0.280	0.380	5.5	7.7	9.5
B6	5.46	16.41	16.13	48	0.00072	0.062	1.238	0.429	0.424	0.0219	0.338	0.211	0.350	0.429	6.6	9.2	10.7
C1	9.12	40.68	39.97	7	0.00358	0.147	0.366	1.673	1.647	0.0992	0.643	0.506	0.628	0.771	11.4	13.2	15.1
C2	7.60	33.90	33.31	20	0.00249	0.122	0.527	1.162	1.144	0.0689	0.563	0.365	0.541	0.735	9.1	11.9	14.7
C3	6.68	29.79	29.28	28	0.00192	0.107	0.682	0.898	0.884	0.0532	0.541	0.296	0.565	0.750	7.9	12.5	15.0
C4	6.08	27.12	26.65	38	0.00159	0.098	0.823	0.744	0.732	0.0441	0.438	0.257	0.430	0.582	7.1	10.2	12.7
C5	4.86	21.68	21.30	41	0.00102	0.078	1.289	0.475	0.468	0.0282	0.382	0.272	0.387	0.488	7.5	9.6	11.3
C6	4.56	20.34	19.99	60	0.00090	0.073	1.464	0.418	0.412	0.0248	0.322	0.211	0.284	0.398	6.2	7.7	9.8
D1	7.28	15.48	21.50	65	0.00120	0.109	0.941	1.101	1.035	0.0552	0.293	0.194	0.278	0.367	6.0	7.7	9.6
D2	5.46	11.61	16.13	85	0.00067	0.081	1.672	0.619	0.582	0.0311	0.220	0.148	0.189	0.264	4.7	5.8	7.7
D3	4.55	9.68	13.44	91	0.00047	0.106	3.769	0.430	0.404	0.0216	0.205	0.127	0.177	0.243	4.3	5.8	7.1
D4	4.10	8.71	12.10	95	0.00038	0.096	4.654	0.294	0.286	0.0133	0.152	0.092	0.126	0.170	3.1	4.3	5.6
D5	3.64	7.74	10.75	96	0.00030	0.054	3.763	0.232	0.226	0.0105	0.185	0.113	0.180	0.230	3.7	5.6	7.0
D6	3.64	7.74	10.75	95	0.00030	0.085	5.890	0.232	0.226	0.0105	0.201	0.147	0.178	0.246	4.7	5.6	7.5
D7	3.64	7.74	10.75	92	0.00030	0.085	5.890	0.232	0.226	0.0105	0.116	0.060	0.086	0.114	1.2	2.8	3.7

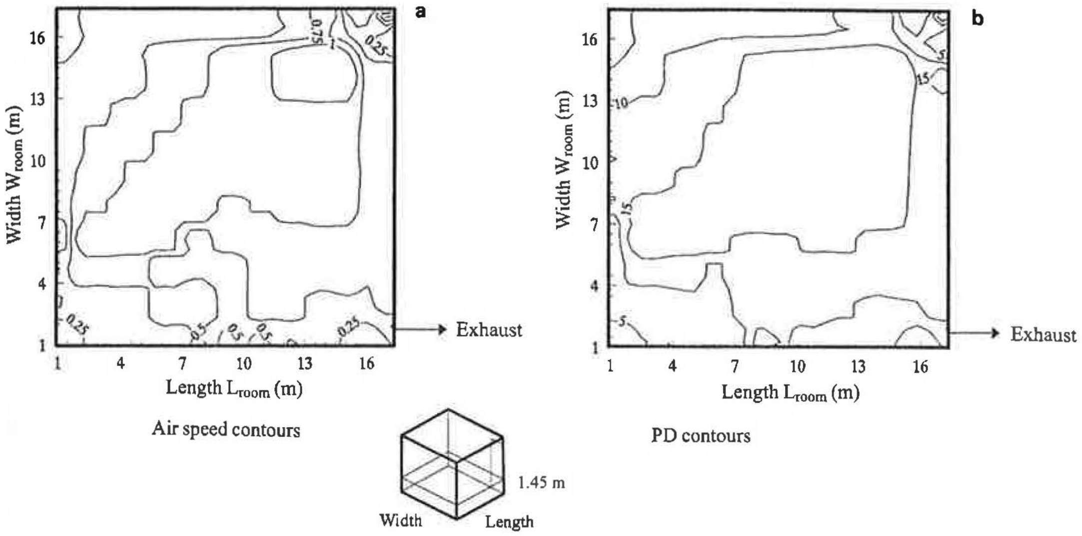

4

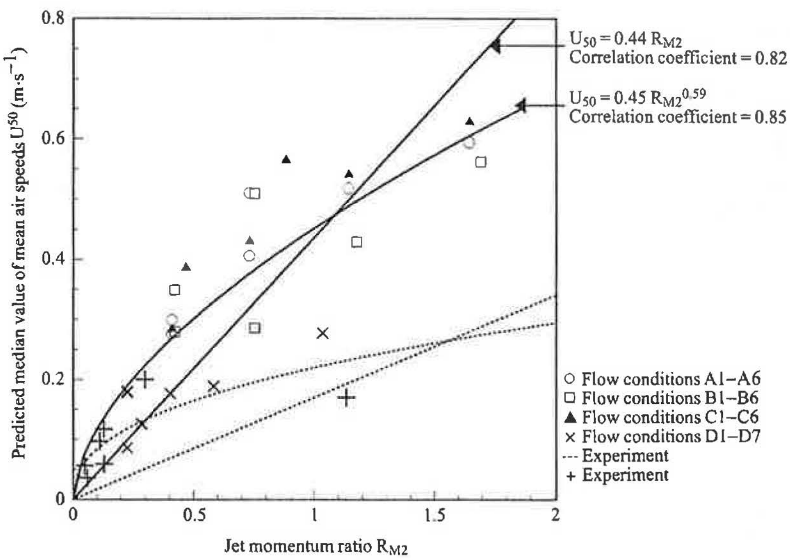

5

Fig. 4. Air speed ($m \cdot s^{-1}$, **a**) and PD (**b**) contours of flow condition A1 at 1.45 m above floor.

Fig. 5. Predicted median value of mean air speeds against jet momentum ratio R_{M2}.

the ventilation rate VR. The predicted mean air speeds including U_{25}, U_{50}, U_{75} and U_{room} using CFD were found to be correlated with the ventilation rate VR in a linear manner. However, this was not the case for the experimental studies reported earlier [7, 10, 11].

The predicted mean air speeds U_{50} were found to be linearly correlated with the modified jet momentum numbers J* as shown in table 5. However, those equations derived from the chamber tests did not have such good agreement as shown in table 6.

The mean air speeds U_{50} did not correlate well with the flow numbers X_1 and X_2 as shown in table 5. Very low correlation coefficients of 0.66 and 0.77 were found, respectively.

The mean air speeds U_{50} did correlate well with the jet momentum ratios R_{M1}, R_{M2} and R_{M3} as shown in table 5. The correlated mean air speeds U_{50} and the simulated jet momentum ratio R_{M2} matched well with the experimental data as shown in figure 5 while the other two agreed reasonably with experiments.

Table 5. Correlation relationships derived from CFD

Fitted equation	Correlation coefficient	Comment
$U_{room} = 0.019$ ACH	0.83	good
$U_{room} = 0.018$ VR	0.92	good
$U_{room} = 262$ J*	0.83	good
$U_{room} = 10.5$ $J^{*0.48}$	0.88	good
$U_{room} = 4.04\ X_1$	0.70	fair
$U_{room} = 0.28\ X_2^{-1}$	0.69	fair
$U_{room} = 0.41\ X_2^{-0.35}$	0.76	fair
$U_{room} = 0.44\ R_{M1}$	0.84	good
$U_{room} = 0.47\ R_{M1}^{0.56}$	0.87	good
$U_{room} = 0.46\ R_{M2}$	0.85	good
$U_{room} = 0.47\ R_{M2}^{0.57}$	0.87	good
$U_{room} = 8.41\ R_{M3}$	0.86	good
$U_{room} = 2.35\ R_{M3}^{0.55}$	0.88	good
$U_{50} = 0.018$ ACH	0.84	good
$U_{50} = 0.017$ VR	0.91	good
$U_{50} = 252$ J*	0.83	good
$U_{50} = 12.2$ $J^{*0.51}$	0.87	good
$U_{50} = 3.85\ X_1$	0.66	fair
$U_{50} = 0.28\ X_2^{-1}$	0.71	fair
$U_{50} = 0.39\ X_2^{-0.38}$	0.77	fair
$U_{50} = 0.43\ R_{M1}$	0.82	good
$U_{50} = 0.44\ R_{M1}^{0.58}$	0.84	good
$U_{50} = 0.44\ R_{M2}$	0.82	good
$U_{50} = 0.45\ R_{M2}^{0.59}$	0.85	good
$U_{50} = 8.07\ R_{M3}$	0.84	good
$U_{50} = 2.41\ R_{M3}^{0.57}$	0.86	good
$PD_{50} = 0.46$ ACH	0.65	fair
$PD_{50} = 0.44$ VR	0.81	good
$PD_{50} = 6191$ J*	0.67	fair
$PD_{50} = 117$ $J^{*0.17}$	0.74	fair
$PD_{50} = 99.8\ X_1$	0.65	fair
$PD_{50} = 6.66\ X_2^{-1}$	0.50	fair
$PD_{50} = 10.2\ X_2^{-0.25}$	0.60	fair
$PD_{50} = 10.8\ R_{M1}$	0.77	fair
$PD_{50} = 11.3\ R_{M1}^{0.47}$	0.80	good
$PD_{50} = 11.0\ R_{M2}$	0.77	fair
$PD_{50} = 11.5\ R_{M2}^{0.41}$	0.80	good
$PD_{50} = 202\ R_{M3}$	0.75	fair
$PD_{50} = 41.1\ R_{M3}^{0.44}$	0.79	fair

For relationships with PD_{50}, only those correlation equations with VR, R_{M1} and R_{M2} have 'good' grades as shown in table 5. The equations with these three macroscopic flow numbers correlate well with the air speeds and the PD.

Comparison with Experimental Data on Air Speed

The correlation equations for room mean air speeds U_{50} and U_{room} derived with the macroscopic flow numbers were compared with those values measured experimentally [7, 10, 11].

Table 6. Correlation relationships derived from experiments

Fitted equation	Correlation coefficient	Comment
$U_{room} = 0.0029$ ACH	0.46	poor
$U_{room} = 0.0057$ VR	0.36	poor
$U_{room} = 37.9$ J*	0.31	poor
$U_{room} = 0.026$ $J^{*-0.27}$	0.48	unphysical
$U_{room} = 0.082\ R_{M1}$	0.76	fair
$U_{room} = 0.19\ R_{M1}^{0.27}$	0.73	fair
$U_{room} = 0.18\ R_{M2}$	0.85	good
$U_{room} = 0.24\ R_{M2}^{0.31}$	0.86	good
$U_{room} = 1.88\ R_{M3}$	0.83	good
$U_{room} = 0.57\ R_{M3}^{0.40}$	0.81	good
$U_{50} = 0.0021$ ACH	0.51	fair
$U_{50} = -0.032$ VR	0.40	unphysical
$U_{50} = 28.9$ J*	0.38	poor
$U_{50} = 0.007$ $J^{*-0.44}$	0.60	unphysical
$U_{50} = 0.077\ R_{M1}$	0.80	good
$U_{50} = 0.16\ R_{M1}^{0.36}$	0.78	fair
$U_{50} = 0.17\ R_{M2}$	0.88	good
$U_{50} = 0.22\ R_{M2}^{0.42}$	0.90	good
$U_{50} = 1.74\ R_{M3}$	0.84	good
$U_{50} = 0.68\ R_{M3}^{0.53}$	0.83	good

PD_{50} from CFD was calculated at different temperatures, not included in the comparison.

The percentage deviation PD_{ev} of the values ϕ_{CFD} (ϕ can be U_{room} and U_{50}) using CFD correlation equations away from those ϕ_{Exp} from experimental data were calculated as:

$$PD_{ev} = \frac{\phi_{CFD} - \phi_{Exp}}{\phi_{Exp}} \times 100\% \quad (12)$$

Values of PD_{ev} are shown in table 7 for linear equations and table 8 for non-linear equations for all those data ϕ_{Exp} determined experimentally. Positive values of PD_{ev} indicate an over-prediction of the mean air speed as compared with the measured data. The calculated PD_{ev} indicates how good is using the correlation equation derived from CFD in predicting the mean air speeds.

From table 7, a large deviation was found in using ACH to predict mean air speeds. The value of PD_{ev} increased as the ACH increased and could go up to 10 times the measured value. For the predicted correlation equation for VR, an underestimation of mean air speeds at low VR and an overestimation of mean air speeds at high VR were found.

Table 7. Comparison of linear correlation equations from experimental data and CFD

Linear equation	Room mean air speed U_{room} measured $m \cdot s^{-1}$	Room mean air speed U_{room} predicted $m \cdot s^{-1}$	Room mean air speed U_{room} PD_{ev} %	Median value of air speed U_{50} measured $m \cdot s^{-1}$	Median value of air speed U_{50} predicted $m \cdot s^{-1}$	Median value of air speed U_{50} PD_{ev} %
ACH, $n \cdot h^{-1}$						
1.63	0.207	0.031	−85	0.200	0.029	−85
4.12	0.343	0.078	−77	0.320	0.074	−77
5.24	0.157	0.100	−37	0.170	0.094	−45
16.10	0.072	0.306	325	0.036	0.290	705
23.00	0.130	0.437	236	0.059	0.414	602
39.40	0.071	0.749	954	0.056	0.709	1,166
50.80	0.130	0.965	642	0.097	0.914	843
62.40	0.149	1.186	696	0.117	1.123	860
Median value of deviation			281			653
VR, $dm^3 \cdot s^{-1} \cdot m^{-2}$						
3.26	0.207	0.059	−72	0.200	0.055	−72
8.01	0.343	0.144	−58	0.320	0.136	−57
8.08	0.157	0.145	−7	0.170	0.137	−19
9.38	0.072	0.169	135	0.036	0.159	343
13.42	0.130	0.241	86	0.059	0.228	287
22.98	0.071	0.414	483	0.056	0.391	598
29.64	0.130	0.534	310	0.097	0.504	420
36.40	0.149	0.655	340	0.117	0.619	429
Median value of deviation			110			315
*J**						
0.00033	0.157	0.086	−45	0.170	0.083	−51
0.00045	0.343	0.118	−66	0.320	0.113	−65
0.00103	0.072	0.269	274	0.036	0.259	620
0.00130	0.207	0.341	65	0.200	0.328	64
0.00219	0.130	0.572	340	0.059	0.551	833
0.00219	0.071	0.572	706	0.056	0.551	883
0.00429	0.130	1.124	765	0.097	1.081	1,015
0.00567	0.149	1.486	897	0.117	1.429	1,121
Median value of deviation			307			
X_1						
0.0547	0.157	0.221	41	0.170	0.211	24
0.1410	0.343	0.570	66	0.320	0.543	70
0.3340	0.207	1.349	552	0.200	1.286	543
Median value of deviation			66			70

Linear equation	Room mean air speed U_{room} measured $m \cdot s^{-1}$	Room mean air speed U_{room} predicted $\cdot s^{-1}$	Room mean air speed U_{room} PD_{ev} %	Median value of air speed U_{50} measured $m \cdot s^{-1}$	Median value of air speed U_{50} predicted $m \cdot s^{-1}$	Median value of air speed U_{50} PD_{ev} %
X_2						
1.09	0.207	0.257	24	0.200	0.257	28
1.24	0.343	0.226	−34	0.320	0.226	−29
1.38	0.157	0.203	29	0.170	0.203	19
Median value of deviation			29			28
R_{M1}, $m^3 \cdot s^{-2}$						
0.1163	0.071	0.051	−28	0.056	0.050	−11
0.1421	0.072	0.063	−13	0.036	0.061	70
0.1715	0.207	0.075	−64	0.200	0.074	−63
0.2692	0.130	0.118	−9	0.097	0.116	19
0.3111	0.149	0.137	−8	0.117	0.134	14
0.3117	0.130	0.137	5	0.059	0.134	127
2.8854	0.157	1.270	709	0.170	1.241	630
3.9653	0.343	1.745	409	0.320	1.705	433
Median value of deviation			21			66
R_{M2}, $m^3 \cdot s^{-2}$						
0.0481	0.071	0.022	−69	0.056	0.021	−62
0.0588	0.072	0.027	−62	0.036	0.026	−28
0.1113	0.130	0.051	−61	0.097	0.049	−50
0.1287	0.149	0.059	−60	0.117	0.057	−52
0.1289	0.130	0.059	−54	0.059	0.057	−4
0.2992	0.207	0.138	−34	0.200	0.132	−34
1.1330	0.157	0.521	232	0.170	0.499	193
2.0350	0.343	0.936	173	0.320	0.895	180
Median value of deviation			62			51
R_{M3}, $m^2 \cdot s^{-2}$						
0.0108	0.071	0.091	28	0.056	0.087	56
0.0133	0.072	0.111	55	0.036	0.107	197
0.0215	0.207	0.181	−13	0.200	0.174	−13
0.0251	0.130	0.211	62	0.097	0.203	109
0.0291	0.149	0.245	64	0.117	0.235	101
0.0291	0.130	0.244	88	0.059	0.235	297
0.1175	0.157	0.988	529	0.170	0.948	458
0.1940	0.343	1.632	376	0.320	1.566	389
Median value of deviation			63			153

Values of the predicted and measured mean air speeds using the correlation equations of the modified jet momentum number J* are shown in tables 7 and 8 for linear and non-linear equations. An overestimation of the mean air speed was found for J* larger than 0.00103.

Results for the flow numbers X_1 and X_2 are also listed in tables 7 and 8. There were only three samples available so the comparisons were limited. Further experimental studies are recommended for a better evaluation of the correlation equations.

Mean air speeds were calculated using the correlation equations with the jet momentum ratios R_{M1}, R_{M2} and R_{M3} in the tables. For predicting the room mean air speed U_{room}, a better agreed value was found in using the non-linear correlation equation of R_{M2}. Good agreement for the room mean air speeds was found for the range of R_{M2} from 0.0481 to 0.2992 with the deviation being 30–70%. Outside this range, the room mean air speeds were over-predicted with a deviation up to 200%, when the range of R_{M2} was from 1.133 to 2.035.

For predicting the median value of mean air speeds, the best agreement was found for the linear correlation equation of R_{M2}. The median value of mean air speeds U_{50} would be under-estimated if the range of R_{M2} was between 0.0481 and 0.2992, with the deviation between 4 and 62%. Larger errors were found for higher values of R_{M2} as shown in table 7.

Comparison with Correlation Equations for Air Speeds Derived Experimentally

The correlation equation derived for CFD shown in table 5 can be compared with those derived from experiments [7, 9–13] shown in table 6. For comparing linear equations for a variable ϕ (U_{room} or U_{50}) with a flow number F (one of ACH, VR, J*, R_{M1}, R_{M2} or R_{M3}):

$$\phi_{CFD} = m_{CFD} F \tag{13}$$

$$\phi_{Exp} = m_{Exp} F \tag{14}$$

The mean percentage of deviation is given by the slopes of the equations m_{CFD} and m_{Exp}:

$$PD_{ev} = \frac{m_{CFD} - m_{Exp}}{m_{Exp}} \times 100\% \tag{15}$$

Results of those expressions for ACH, VR, J*, R_{M1}, R_{M2} and R_{M3} are shown in table 9. Again, R_{M2} has the best correlation equation with the local air speeds.

For comparison with non-linear equations, the mean values of PD_{ev} are calculated from equation 12 for a range of flow numbers taking the common design values. Values of PD_{ev} for non-linear equations are shown in table 10. R_{M2} is the best parameter correlated with the mean air speeds in the occupied zone. Plotting U_{50} against R_{M2} in figure 5 illustrates their relationships.

Table 8. Comparison of non-linear correlation equations from experimental data and CFD

Non-linear equation	Room mean air speed U_{room}			Median value of air speed U_{50}		
	measured $m \cdot s^{-1}$	predicted $m \cdot s^{-1}$	PD_{ev} %	measured $m \cdot s^{-1}$	predicted $m \cdot s^{-1}$	PD_{ev} %
*J**						
0.00033	0.157	0.224	43	0.170	0.205	20
0.00045	0.343	0.260	−24	0.320	0.240	−25
0.00103	0.072	0.386	437	0.036	0.365	914
0.00130	0.207	0.432	109	0.200	0.412	106
0.00219	0.130	0.555	327	0.059	0.536	809
0.00219	0.071	0.555	681	0.056	0.536	858
0.00429	0.130	0.767	490	0.097	0.757	680
0.00567	0.149	0.877	488	0.117	0.872	646
Median value of deviation			382			663
X_2						
1.09	0.207	0.398	92	0.200	0.377	89
1.24	0.343	0.380	11	0.320	0.359	12
1.38	0.157	0.366	133	0.170	0.345	103
Median value of deviation			92			89
R_{M1}, $m^3 \cdot s^{-2}$						
0.1163	0.071	0.141	98	0.056	0.126	126
0.1421	0.072	0.158	119	0.036	0.142	294
0.1715	0.207	0.175	−15	0.200	0.158	−21
0.2692	0.130	0.225	73	0.097	0.206	112
0.3111	0.149	0.244	64	0.117	0.224	91
0.3117	0.130	0.245	88	0.059	0.224	279
2.8854	0.157	0.851	442	0.170	0.814	379
3.9653	0.343	1.017	196	0.320	0.978	206
Median value of deviation			93			166
R_{M2}, $m^3 \cdot s^{-2}$						
0.0481	0.071	0.083	17	0.056	0.075	34
0.0588	0.072	0.093	30	0.036	0.085	135
0.1113	0.130	0.134	3	0.097	0.123	27
0.1287	0.149	0.146	−2	0.117	0.134	15
0.1289	0.130	0.146	12	0.059	0.134	128
0.2992	0.207	0.236	14	0.200	0.221	10
1.1330	0.157	0.505	221	0.170	0.484	185
2.0350	0.343	0.705	105	0.320	0.684	114
Median value of deviation			16			74
R_{M3}, $m^2 \cdot s^{-2}$						
0.0108	0.071	0.195	175	0.056	0.183	226
0.0133	0.072	0.218	203	0.036	0.205	469
0.0215	0.207	0.284	37	0.200	0.270	35
0.0251	0.130	0.310	138	0.097	0.295	204
0.0291	0.149	0.336	125	0.117	0.321	174
0.0291	0.130	0.336	158	0.059	0.321	444
0.1175	0.157	0.724	361	0.170	0.711	318
0.1940	0.343	0.954	178	0.320	0.946	196
Median value of deviation			167			215

Discussion

A new area of application for CFD [16–18] has been demonstrated. Four sets of simulations were performed in rooms of different sizes with a common ventilation design and varying arrangements of air supply inlets. A total of 25 numerical experiments under isothermal flow conditions was examined. The geometry of the spaces and the ventilation conditions are typical of designs used in the HKSAR, but it should be borne in mind that any such ventilation system would be operated with a high number of ACH.

The CFD package employed was developed in-house so that operating and input conditions could be changed easily. Advantages of this programme are that it has the flexibility of using different turbulence models, different discretization schemes and different algorithms for solving the velocity-pressure-linked equations.

Correlation relationships among the mean air speeds U_{50}, U_{mean} and the PD_{50} with 10 macroscopic flow numbers were derived. The 10 macroscopic flow numbers are: the total ventilation rate Q; ACH; VR; ADPI; J*; 2 new flow numbers, X_1 and X_2, and 3 expressions of the jet momentum ratio R_{M1}, R_{M2} and R_{M3}.

The correlation equations deduced from the technique of CFD have been compared with those correlation equations derived from experiments using 'real' measurements reported in earlier studies. The result of this is that the jet momentum ratio R_{M2} [13, 14, 23], given by equation 5, has been found to be a good parameter for relating the mean air speeds and PD in the occupied zone. The correlation equation relating mean air speeds with R_{M2} was found to agree with the experimental data for the range of R_{M2} between 0.0481 and 0.2992. As a consequence of this the equations for R_{M2} in table 5 are recommended for use in ventilation design.

Table 9. Comparison between linear correlation equations derived from experiment and CFD

Macroscopic flow parameter	Room mean air speed U_{room}			Median value of mean air speeds U_{50}		
	slope (experiment) m_{Exp}, n	slope (CFD) m_{CFD}, n	deviation PD_{ev}, %	slope (experiment) m_{Exp}, n	slope (CFD) m_{CFD}, n	deviation PD_{ev}, %
ACH	0.0029	0.019	555	0.0021	0.018	757
VR	0.0057	0.018	216	–0.032	0.017	–153
J*	37.9	0.83	–98	28.9	252	772
R_{M1}	0.082	0.44	437	0.077	0.43	458
R_{M2}	0.18	0.46	156	0.17	0.44	159
R_{M3}	1.88	8.41	347	1.74	8.07	364

Table 10. Comparison between non-linear correlation equations derived from experiment and CFD

Macroscopic flow parameter	Lower limit of flow number	Upper limit of flow number	Mean deviation for predicting U_{room} PD_{ev}, %	Mean deviation for predicting U_{50} PD_{ev}, %
J*	0.00033	0.00567	399	593
R_{M1}	0.11630	3.96530	187	206
R_{M2}	0.04810	2.03500	87	97
R_{M3}	0.01080	0.19400	184	220

Appendix

Nomenclature

A	area (m^2)
ACH	air changes per hour, (n)
ADPI	air diffusion performance index (%)
D	distance (m)
F	flow number: one of ACH, VR, R_{M1}, R_{M2}, or R_{M3}
g	gravity (9.81 $m \cdot s^{-2}$)
H	height (m)
H_b	height of the diffuser above the floor level (m)
J*	modified jet momentum number
L	length (m)
m	slope
N_{in}	number of inlet
P	pressure (Pa)
PD	percentage of people dissatisfied with the air draught (%)
PD_{ev}	percentage deviation (%)
Q	total ventilation flow rate ($m^3 \cdot s^{-1}$, $kg \cdot s^{-1}$ as specified)
R	range of diffuser (m)
R_M	jet momentum ratio
S_d	separation distance of diffusers (m)
T	temperature (°C)
Tu	turbulence intensity (%)
u, v, w	mean velocity components in the Cartesian co-ordinate direction x, y, z, respectively ($m \cdot s^{-1}$)
U	mean air speed ($m \cdot s^{-1}$)
V	volume (m^3)
W	width (m)
VR	ventilation rate per unit floor area ($dm^3 \cdot s^{-1} \cdot m^{-2}$)
x, y, z	co-ordinate system
X_1, X_2	flow numbers
ϕ, ϕ_t, ϕ'	mean, instantaneous and fluctuating values of the flow property ϕ, respectively
τ_p	control volume at a point p
z	horizontal distance from a jet (m)

Subscripts

None	initial condition
1, 2, 3	condition 1, condition 2, condition 3
25, 50, 75	the first, the median and the third quartile values, respectively
a	of air
b	below air inlet
CFD	values calculated by computational fluid dynamics
Exp	experimental value
i, j, k	the ith, jth and kth numbers
io	between inlet and outlet
in	inlet condition, of inlet
ip	between inlet and occupied zone
op	between outlet and occupied zone
ou	outlet condition, of outlet
p	at nodal point
room	of room

References

1 CIBSE Guides: Installation and Equipment Data. London, CIBSE, 1986.

2 ASHRAE Handbook: Fundamentals 1997. Atlanta, American Society of Heating, Refrigerating and Air-Conditioning Engineers, 1997.

3 ASHRAE Handbook: Applications 1995. Atlanta, American Society of Heating, Refrigerating and Air-Conditioning Engineers, 1995.

4 ASHRAE: Standard 62-1989: Ventilation for acceptable indoor air quality. Atlanta, American Society of Heating, Refrigerating and Air-Conditioning Engineers, 1989.

5 European Concerted Action: Indoor air quality and its impact on man. Report No 11: Guidelines for ventilation requirements in buildings. Luxembourg, Office for Publications of the European Communities, 1992.

6 ISO: Standard 7730: Moderate thermal environments – Determination of the PMV and PPD indices and specification of the conditions for thermal comfort. Geneva, International Standards Organization, 1994.

7 Fung WY: Numerical Studies on the Air Flow and Assessment of Thermal Comfort Indices Related to Draught in Air-Conditioned and Mechanical Ventilated Spaces; PhD thesis, Department of Building Services Engineering, The Hong Kong Polytechnic University, 1995.

8 Ogilvie JR, Barber EM: Jet momentum number: An index of air velocity at floor level. Building Systems: Room Air and Air Contaminant Distribution. Atlanta, American Society of Heating, Refrigerating and Air-Conditioning Engineers, 1989, pp 211–214.

9 Wong LT: A Study on the Building Air Flow Induced by Environmental Control Systems and Characteristics of Air Diffusion Devices; PhD thesis, Department of Building Services Engineering, Hong Kong Polytechnic University, 1997.

10 Chow WK, Wong LT: Experimental studies on the air flow characteristics included by a high-sidewall grill in a climate chamber. Indoor Built Environ 1996;5:82–98.

11 Chow WK, Wong LT, Fung WY: Field measurement in the air flow characteristics of big mechanically ventilated spaces. Building Environ 1996;31:541–550.

12 Chow WK, Wong LT: Local air speeds measurement in mechanically ventilated spaces. Building Environ, accepted for publication.

13 Chow WK, Wong LT: Air diffusion terminal devices: Macroscopic numbers describing jet momentum. Building Services Eng Res Technol 1998;19:49–54.

14 Li ZH, Zhivov AM, Zhang JS, Christiansen LL: Characteristics of diffuser air jets and airflow in the occupied regions of mechanically ventilated rooms – A literature review. ASHRAE Trans 1993;99(part 1):1119–1127.

15 Fanger PO, Melikov AK, Hanzawa H, Ring J: Air turbulence and sensation of draught. Energy Buildings 1988;12:21–39.

16 Moser A: Numerical simulation of room thermal convection – Review of IEA Annex 20 results. Proc Int Symp Room Air Convection and Ventilation Effectiveness, Tokyo, Heating, Air-Conditioning and Sanitary Engineers of Japan, 1992, pp 77–86.

17 Schild PG, Tjelflaat PO, Aiulfi D: Guidelines for CFD modelling of atria. ASHRAE Trans Symp 1995;101(part 2):1311–1332.

18 Chow WK, Fung WY: Numerical studies on the indoor air flow in the occupied zone of ventilated and air-conditioned space. Building Environ 1996;31:319–344.

19 Chow WK: Numerical studies on air-conditioned space. Proc ASHRAE Far East Conference: Air-Conditioning in Hot Climates, Kuala Lumpur, October 1989, pp 43–55.

20 Chow WK: Application of computational fluid dynamics in building services engineering (paper 32-02). Natl Conf in Heating, Ventilation and Air-Conditioning, Fozhou, November 1998.

21 Ko NWN, Chen ASK: In the intermixing region behind circular cylinders with stepwise change of the diameter. Exp Fluid 1990;9:213–221.

22 Brüel & Kjær: Instruction Manual – Indoor Climate Analyzer Type 1213. Nærum, Brüel & Kjær, 1990.

23 Zhivov AM: Theory and practice of air distribution with included jets. ASHRAE Trans 1993;99(part 1):1152–1159.